

Quenched chirality in RbNiCl_3

Maikel C. Rheinstädter* and Mechthild Enderle

*Institut Laue-Langevin, 6 rue Jules Horowitz, BP 156,38042 Grenoble Cedex 9, France and
Technische Physik, Universität des Saarlandes, PSF 1551150, 66041 Saarbrücken, Germany*

Garry J. McIntyre

Institut Laue-Langevin, 6 rue Jules Horowitz, BP 156,38042 Grenoble Cedex 9, France

(Dated: January 3, 2022)

The critical behaviour of stacked-triangular antiferromagnets has been intensely studied since Kawamura predicted new universality classes for triangular and helical antiferromagnets. The new universality classes are linked to an additional discrete degree of freedom, chirality, which is not present on rectangular lattices, nor in ferromagnets. However, the theoretical as well as experimental situation is discussed controversially, and generic scaling without universality has been proposed as an alternative scenario. Here we present a careful investigation of the zero-field critical behaviour of RbNiCl_3 , a stacked-triangular Heisenberg antiferromagnet with very small Ising anisotropy. From linear birefringence experiments we determine the specific heat exponent α as well as the critical amplitude ratio A^+/A^- . Our high-resolution measurements point to a single second order phase transition with standard Heisenberg critical behaviour, contrary to all theoretical predictions. From a supplementary neutron diffraction study we can exclude a structural phase transition at T_N . We discuss our results in the context of other available experimental results on RbNiCl_3 and related compounds. We arrive at a simple intuitive explanation which may be relevant for other discrepancies observed in the critical behaviour of stacked-triangular antiferromagnets. In RbNiCl_3 the ordering of the chirality is suppressed by strong spin fluctuations, yielding to a different phase diagram, as compared to e.g. CsNiCl_3 , where the Ising anisotropy prevents these fluctuations.

PACS numbers: 75.25.+z, 75.50.Ee, 75.40.Gb, 75.10.Jm,

Keywords: spin systems; spin fluctuations; rubidium compounds

On a hexagonal lattice, an antiferromagnet can never entirely satisfy its interactions, they will be at least partially frustrated. A stacked set of triangular planes will nevertheless develop long-range order for any finite inter-plane interaction. In the perfectly isotropic case (Heisenberg antiferromagnet), neighboring spins on a triangle compromise the antiferromagnetic interaction by including 120° , along the hexagonal axis the spins will be collinear. The magnetic structure is then defined by two continuous degrees of freedom (the polar and azimuthal angle of one chosen spin) and one additional discrete degree of freedom, the chirality, the sense of rotation of the spin direction on a chosen triangle. This chirality vanishes in collinear structures, on rectangular lattices and in ferromagnets. It is still present for easy-plane antiferromagnets, and in the spin-flop phases of antiferromagnets with a small Ising-anisotropy. A large family of hexagonal compounds with a chiral degree of freedom can be described by the Hamiltonian

$$H = J \sum_{i,j}^{\text{intra chain}} \mathbf{S}_i \cdot \mathbf{S}_j + J' \sum_{i,k}^{\text{inter chain}} \mathbf{S}_i \cdot \mathbf{S}_k - D \sum_i (S_i^z)^2. \quad (1)$$

Here, $J > 0$ denotes the antiferromagnetic exchange interaction between nearest neighbours along the symmetry axis, $J' > 0$ the antiferromagnetic interaction between nearest neighbours on a triangle. The single ion anisotropy constant D favors an easy-axis ($D > 0$) or plane ($D < 0$). Kawamura¹ predicted that the chiral de-

gree of freedom provokes not only a different topology of the field-temperature phase diagrams, but also new types of universal critical behaviour, the $n = 2$ chiral and the $n = 3$ chiral universality classes. This prediction is discussed controversially, and arguments have been given for quite different scenarios, as e.g. generic non-universal behavior². Table I lists Kawamura's predictions for the critical exponents α , β , γ and δ and the ratio A^+/A^- for antiferromagnets on rectangular and triangular lattices as a survey.

ABX_3 compounds with easy-axis anisotropy, as CsNiCl_3 , RbNiCl_3 , CsMnI_3 and CsNiBr_3 are well described by the Hamiltonian in Eq. (1) and have developed into model systems for low dimensional fluctuations and ordering, see e.g. [3] for a recent review. These compounds show quasi one-dimensional (1D) magnetic behavior, because the intrachain interaction J is much larger than the interchain interaction J' , typically $J'/J \approx 10^{-2}$. One-dimensional short-range antiferromagnetic order within the 1D spin chains develops below about 40 K. At lower temperatures there is a phase transition into a three-dimensionally (3D) magnetically ordered structure. Without an external field, Heisenberg antiferromagnets with an Ising anisotropy on a triangular lattice undergo two successive phase transitions, where ordering of the spin components parallel and perpendicular to the hexagonal c -axis occurs at T_{N1} and T_{N2} ($< T_{N1}$), respectively. Below T_{N2} , the spins form a 120° structure in the ac plane. The predicted B-T phase diagram is schematically shown in Fig. 1. The two zero-field

		α	β	γ	ν	A^+/A^-
\square	Ising	0.1098(29)	0.325(1)	1.2402(9)	0.6300(8)	0.55
	XY	-0.0080(32)	0.346(1)	1.3160(12)	0.6693(10)	0.99
	Heisenberg	-0.1160(36)	0.3647(12)	1.3866(12)	0.7054(11)	1.36
\triangle	n=2 chiral	0.34(6)	0.253(10)	1.13(5)	0.54(2)	0.36(2)
	n=3 chiral	0.24(8)	0.30(2)	1.17(7)	0.59(2)	0.54(2)

TABLE I: Critical exponents for antiferromagnets on square and triangular lattices after Kawamura, see [3,4,5] and references therein.

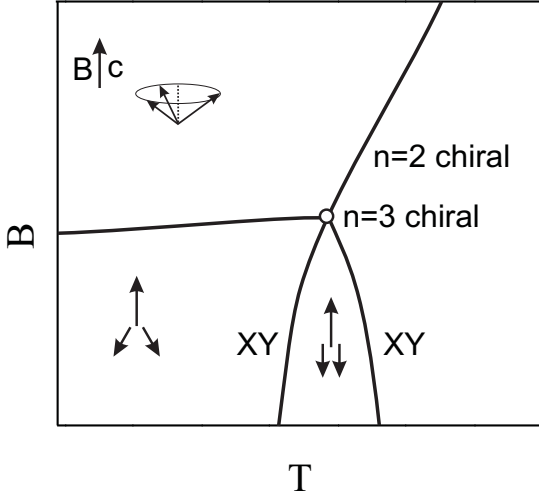


FIG. 1: Predicted phase diagram for ABX_3 with easy-axis anisotropy. In zero magnetic field, two successive phase transitions are expected, connected with ordering of the spin components parallel and perpendicular to the hexagonal c -axis at T_{N1} and T_{N2} ($<T_{N1}$), respectively. Both transitions should show XY critical behavior.

phase transitions should show 3D XY-critical behavior¹. On a rectangular lattice, there is just one transition with Ising-type critical behavior^{3,4,5}.

In order to clarify the number of phase transitions in $RbNiCl_3$, and their criticality, we performed linear magnetic birefringence (LMB) experiments with a high temperature resolution to measure the critical exponent α and the amplitude ratio A^+/A^- . The paper is organized as follows: The properties of $RbNiCl_3$ are discussed in Sect. I. Experimental details of the birefringence set-up are presented in Sect. II, the LMB results and the outcome of a supplementary neutron diffraction study are shown and discussed in Sect. III. The anomalous behavior of $RbNiCl_3$ as compared to other members of the above mentioned ABX_3 family, is discussed in the discussion in Sect. IV.

I. $RbNiCl_3$

$RbNiCl_3$ is a quasi 1D $S=1$ Heisenberg antiferromagnet with a weak Ising anisotropy on a triangular lattice

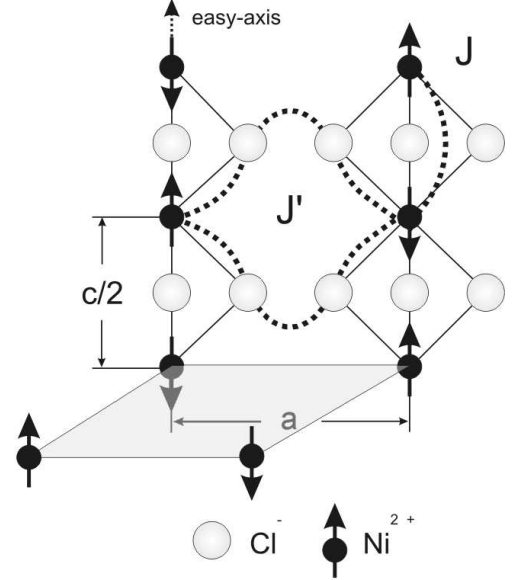


FIG. 2: In $RbNiCl_3$ magnetic exchange J along the easy-axis is two orders of magnitude larger than exchange in the basal plane J' , which involves two Cl^- -ions (as compared to one along c).

(hexagonal space group $P6_3/mmc$). As in other members of the ABX_3 family, $CsNiCl_3$, $CsMnI_3$, $CsNiBr_3$ and $RbNiBr_3$, the magnetic Ni^{2+} -ions form strongly coupled chains along the crystallographic c -axis. The chains are characterized by an intrachain exchange parameter J , which is much larger than the interchain exchange parameter J' because magnetic exchange in the basal plane is mediated via two X-ions compared to only one along c , as pictured in Fig. 2. $J'/J = 0.38K/23.8K = 1.6 \cdot 10^{-2}$ in $RbNiCl_3$ ⁶. The magnetic behavior therefore is quasi 1D. At $T_N \simeq 11$ K, there is a phase transition into a 3D magnetically ordered structure.

Magnetic ordering in $RbNiCl_3$ can be discussed in the context of other members of the ABX_3 family. In e.g. $CsNiCl_3$, two successive phase transitions are found in neutron scattering, magnetic birefringence and specific heat capacity experiments and display 3D XY-critical behavior with the corresponding critical exponents^{3,18}, as predicted by Kawamura. For $RbNiCl_3$, with most experimental techniques just one transition is observed. The criticality of this transition is not clear: Different meth-

Technique	Ref.	T_N (K)	α	β
neutron diffraction	[7]	11.15		$\beta = 0.30 \pm 0.01$
	[8]	11.11, 11.25		$\beta_{\parallel, \perp} = 0.27 \pm 0.01, 0.28 \pm 0.01$
LMB	[9]	11	0.06 ± 0.04	
	[10]	11.3		
	[11]	11		
NMR	[12]	11.18, 11.36 (?)		
susceptibility, torque	[13, 14]	11.38		
magnetization, susceptibility	[15]	11		
thermal expansion	[16]	11.2		
specific heat capacity	[16, 17]	11.0		

TABLE II: Reported results for the zero-field phase transition in RbNiCl_3 . Values for the relation A^+/A^- are not given in the references.

ods obtained disagreeing values of the critical exponents and accordingly different universality classes have been proposed for the transition. None of the experimentally determined values agrees with the prediction for the 3D XY class. Table II summarizes experimental techniques and the values determined for T_N , α and β , as found in literature. Apart from a neutron scattering study by Oohara *et al.*⁸, all measuring techniques report only one phase transition. The temperature resolution in all experiments was better than 0.02 K, considerably smaller than 0.15 K, claimed as the distance between T_{N1} and T_{N2} in the neutron scattering study. The anomalies in all techniques (except [8]) appear very sharp while the overlap of two close lying divergences would lead to a rounded and broad anomaly. Furthermore, the measured critical exponents do not coincide with the predicted 3D XY-critical behavior. If the two transitions would fall together at the same temperature, the transition from the paramagnetic directly into the chiral ordered state should show $n=3$ chiral exponents, against the experimental evidence.

RbNiCl_3 has a very small Ising anisotropy D , as compared to other members of the ABX_3 family. We argue that the pronounced Heisenberg character plays the key role for the understanding of phase transitions and criticality in RbNiCl_3 . In the next section, we present and discuss the results of our high resolution LMB experiments.

II. EXPERIMENTAL

The linear birefringence $n_{ac} = n_c - n_a$ has been measured using a Sénarmont set-up^{19,20} with a He-Ne laser at $\lambda=632.8$ nm. Before and behind the sample, apertures with a diameter of 0.3 mm were installed. The sensitivity of the Sénarmont set-up was increased by modulating the incoming polarisation with 50 kHz and lock-in detection of the intensity. Single crystals of RbNiCl_3 were grown by the Bridgeman method. The slightly hygroscopic samples were prepared by cleaving in a glovebox under He-atmosphere. The natural cleavage planes con-

tain the c -axis, and correspond probably to $\{10\bar{1}0\}$. The typical sample size was $4 \times 4 \times 1.5$ mm³. The cleft samples were used without further polishing and were mounted stress-free in an optical ⁴He continuous flow cryostat with a temperature stability of 0.001 K. The sample temperature was measured with a Cernox semiconductor thermometer in lock-in technique with a relative accuracy of 0.001 K.

Under certain conditions, the derivative dn_{ac}/dT is proportional to the magnetic part of the specific heat capacity, see e.g. [21] and references therein. This relation is in particular valid close to the phase transitions of the antiferromagnetic triangular ABX_3 compounds with and without easy-axis anisotropy, as CsNiCl_3 and RbNiCl_3 . In the temperature range of the phase transition in RbNiCl_3 at $T_N \approx 11$ K, the specific heat capacity is already dominated by contributions of the crystal lattice. The critical properties of the magnetic specific heat are therefore difficult to measure in a standard specific heat capacity setup. Here the birefringence is an elegant way to determine the critical exponent α as well as the amplitude ratio A^+/A^- of the critical part of the specific heat capacity above and below the phase transition.

III. RESULTS

Figure 3 shows the temperature dependence of n_{ac} over a broad temperature range. At high temperatures, n_{ac} linearly decreases with lowering temperature. Below about $T=70$ K there is distinct deviation from linear behavior due to the onset of short ranged 1D correlations along the Ni-chains⁹. The inset in Fig. 3 shows the temperature range of the 3D phase transition in magnification. The onset of 3D correlations close to $T_N=10.89$ K, which finally leads to a 3D magnetically ordered structure, is indicated by the drop of the birefringence below 11 K.

The derivative of the birefringence with respect to temperature is described by a power law:

$$\frac{dn_{ac}}{dT} = A^{\pm} \left| \frac{T - T_N}{T_N} \right|^{-\alpha^{\pm}}. \quad (2)$$

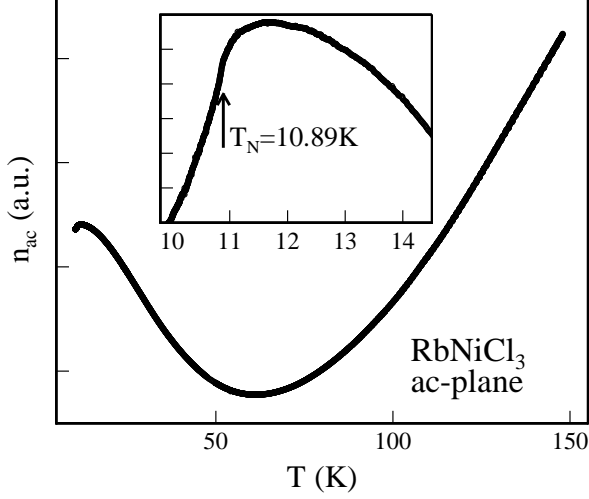


FIG. 3: Temperature dependence of the birefringence $n_{ac} = n_c - n_a$ over a broad temperature range. The inset shows the range of the phase transition in magnification. The transition is marked by an arrow.

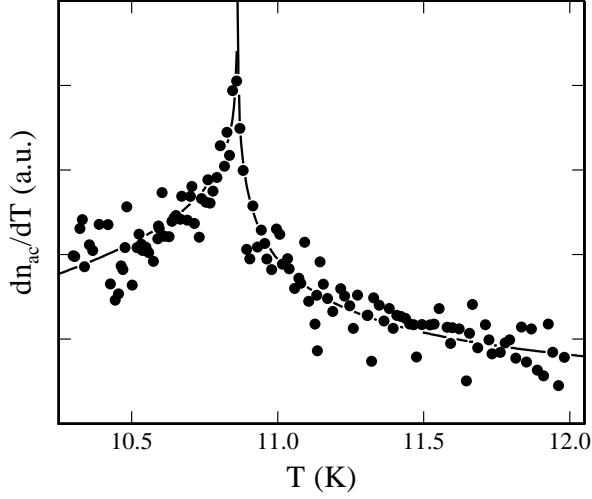


FIG. 4: Temperature-derivative of the critical part of the birefringence, dn_{ac}/dT , which is proportional to the magnetic specific heat. The solid line is the resulting fit with Eq. (2).

Figure 4 shows dn_{ac}/dT , the solid line is a fit after Eq. (2). The noncritical contribution due to 1D correlations and lattice natural birefringence was taken into account by a polynomial of the form $a+bT+cT^2+dT^3+eT^4$ which was subtracted from the data. We observe only one transition as the fitted transition temperatures for the range below and above T_N perfectly coincide. The good temperature resolution allows to measure as close to the phase transition as 10^{-4} in reduced temperature, considerably closer than all previous experiments. Even if two different transition temperatures were allowed for

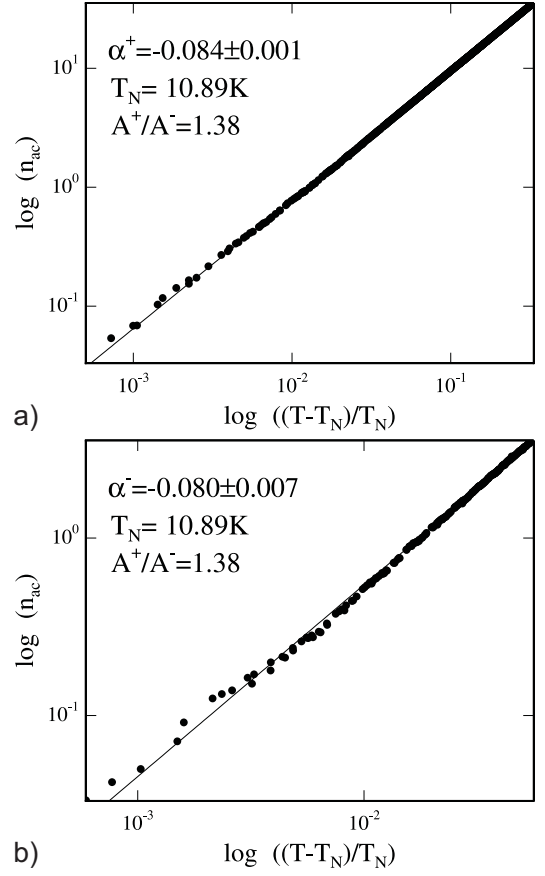


FIG. 5: Log-log plots of the critical part of the birefringence n_{ac} vs. reduced temperature $|t| = |(T - T_N)/T_N|$ for (a) $T > T_N$ and (b) $T < T_N$. Solid lines are fits with Eq. (2), the fitted values for α^\pm , T_N and the ratio A^+/A^- are given in the figure.

the high and the low temperature side, they converge to a single one in the fit. We do not observe any signs of crossover effects. To check the quality of the fits, Fig. 5 shows log-log plots of the critical part of n_{ac} vs. reduced temperature $|t| = |(T - T_N)/T_N|$ for $T \leq T_N$ in the range close to the phase transition. T_N is determined to $T_N = 10.888 \pm 0.001$ K, the values for α from the high and the low temperature side to $\alpha^+ = -0.084 \pm 0.001$ and $\alpha^- = -0.080 \pm 0.007$. The ratio A^+/A^- is obtained to 1.38 ± 0.07 . Comparing these values with those from Tab. I, the determined critical exponent and A^+/A^- agree remarkably well with those of a Heisenberg anti-ferromagnet on the rectangular lattice. Chiral or XY-behavior, as predicted in the chiral theory, can be excluded. Two close lying successive phase transitions that would lead to a rounded anomaly in the measurements can obviously be excluded by our measurements in Figs. 4 and 5.

The unusual behavior of RbNiCl_3 might be explained by a lift of degeneracy of the magnetic exchange interactions in the hexagonal basal plane. This scenario has been discussed for other ABX_3 compounds in e.g. [3,22].

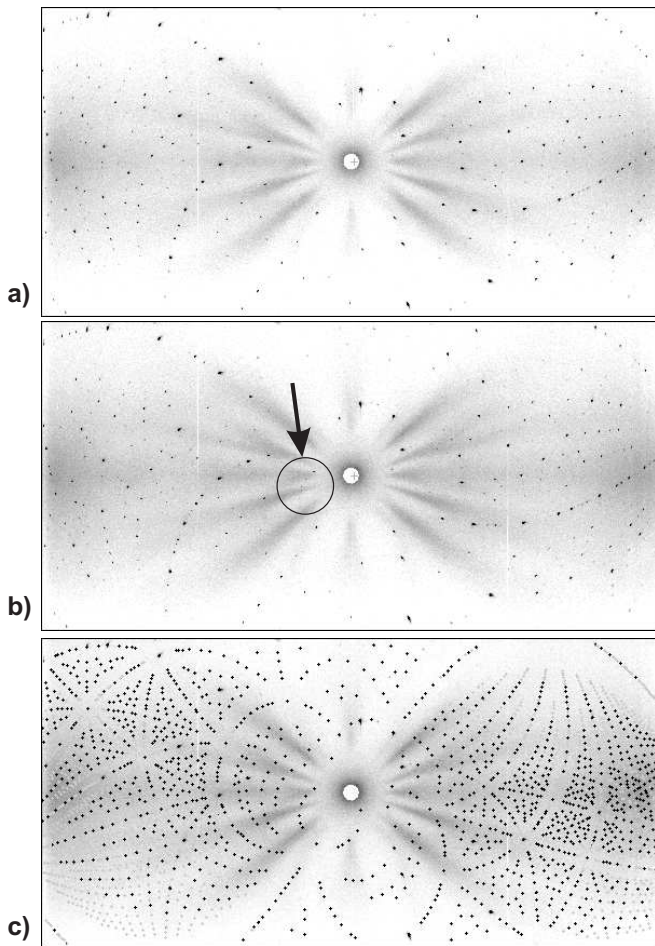


FIG. 6: Laue-photographs taken at different temperatures. (a) $T=20$ K, above phase transition; (b) $T=2$ K, in the magnetically ordered phase (some of the magnetic superlattice reflections are marked by the arrow); (c) $T=2$ K with predicted Laue-pattern.

Considering the crystal structure of RbNiCl_3 , as pictured in Fig. 2, a lift of degeneracy is inseparable from changes in the crystal lattice. We therefore carried out supplementary single-crystal neutron diffraction experiments at the new Vivaldi Laue-diffractometer at the high flux reactor of the ILL in Grenoble, France, to detect a possible change in the lattice symmetry below T_N . Vivaldi's large image plate thereby allows to survey large areas of reciprocal space to detect possible superlattice reflections in the ordered phase. Typical sample crystals of about $1 \times 1 \times 2 \text{ mm}^3$ were mounted in a helium orange cryostat. We took exposures at $T=20$ K, in the paramagnetic, and in the ordered phase, at 2 K. The corresponding Laue patterns are shown in Fig. 6. The reflections of the $T=20$ K exposure in Fig. 6 (a) could be indexed by a primitive hexagonal cell with lattice parameters $a=6.93 \text{ \AA}$ and $c=5.89 \text{ \AA}$. The reflections in the magnetically ordered phase can be described in terms of a tripled hexagonal cell $(a\sqrt{3}, a\sqrt{3}, c)$. We could not detect any splitting of the reflections below the phase transition within the experi-

mental angular resolution of 10° nor the appearance of additional superlattice reflections which are not indexed by the tripled hexagonal cell. Even a small orthorhombic or monoclinic distortion would lead to the appearance of Bragg peaks at former forbidden positions and should have been detected. Our measurements therefore confirm the previous results by Yelon and Cox⁷. Moreover, the zero-field birefringence n_{ab} in the hexagonal basal plane¹⁰ vanishes, which independently excludes any orthorhombic or monoclinic distortion in the ordered phase.

IV. DISCUSSION

The question arises, why RbNiCl_3 - which orders into the same magnetic structure as CsNiCl_3 - does not show two successive phase transitions and the predicted chiral critical behavior. Two successive phase transitions can be excluded from our high resolution birefringence measurements as well as from most of the previously reported experimental results. Close lying divergences due to two close lying phase transition should lead to a rounded anomaly in the measurements. But even in the high resolved data of Fig. 4, the anomaly remains sharp and pronounced confirming the single phase transition observed in a previous LMB study¹⁰ and other techniques (see the listing in Tab II). The critical exponent α and the ratio A^+/A^- correspond to conventional Heisenberg critical behavior and therefore point to a disordered chirality below T_N . A vanishing chirality due to a collinear structure can be excluded from the structural data. If there was only one transition, connected with ordering of the spin components parallel and perpendicular to the 1D axis but no static ordering of the chirality, the corresponding transition should indeed show conventional Heisenberg critical behavior like for antiferromagnets on rectangular lattices. We argue in the following that spin fluctuations suppress long ranged chiral order in RbNiCl_3 below T_N .

The chirality, which basically takes into account the sense of rotation of the spin direction on a chosen triangle, is defined as²³:

$$\vec{\kappa} = \frac{2}{3\sqrt{3}} (\mathbf{S}_i \times \mathbf{S}_j + \mathbf{S}_j \times \mathbf{S}_k + \mathbf{S}_k \times \mathbf{S}_i). \quad (3)$$

Figure 7 shows the ordered spin structure of RbNiCl_3 in the hexagonal basal plane, as proposed in the literature. The spins lie in a $[001][110]$ plane with $2/3$ of the spins canted away from c by an angle θ . θ depends on the ratio D/J' and is determined to $\theta=57.5^\circ$ in RbNiCl_3 , very close to the ideal value of 60° . In this model, the chirality $\vec{\kappa}$ is long ranged ordered and changes sign from one to the neighboring triangle, respectively. Anti-phase domains of the chirality contribute equally in a neutron scattering experiment. Oohara and Iio investigated the $\text{RbNi}_{1-x}\text{Co}_x\text{Cl}_3$ system¹⁴ with LMB. By replacing Ni^{2+} by Co^{2+} , the magnitude of the Ising anisotropy D , which is very small in pure RbNiCl_3 (70 % that of CsNiCl_3), can

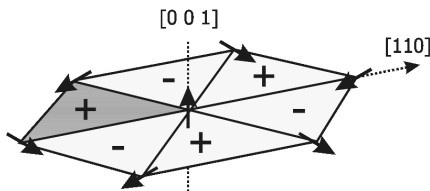


FIG. 7: In the magnetically ordered phase of RbNiCl_3 as proposed in literature, $2/3$ of the spins are canted away from c in the $[110]$ direction. The chirality $\vec{\kappa}$ changes sign from one triangle to the neighboring triangle.

gradually be increased. With increasing D , two anomalies become visible in the LMB experiments and the distance $T_{N1}-T_{N2}$ increases. The latter study clearly shows that the small Ising anisotropy D plays the crucial role for the understanding of criticality and phase transitions in RbNiCl_3 . It also proves that LMB is capable to detect the upper transition, if it exists.

The anisotropy D confines the 120° spin structure in the ac plane. Depending on the ratio D/J' , the structure might exhibit an additional degree of freedom connected with the rotation of the 120° structure in the ac plane. This *quasidegeneracy* has been predicted²⁴ and experimental evidence was found for the case of CsNiCl_3 ²⁵. The energy barrier for a rotation of the spin-star in the ac plane is of the order of $D(D/6J')^2$ [11]. Miyashita²⁴ suggested, this quasidegeneracy exists, if $(D/J') < 1$ ($D/J' = 0.06$ in RbNiCl_3). Even though $D_{\text{RbNiCl}_3} = 0.7D_{\text{CsNiCl}_3}$, $D(D/6J')^2$ for RbNiCl_3 is just 7 % of that of CsNiCl_3 ; the quasidegeneracy should therefore be strongly enhanced in the paramagnetic phase of pure RbNiCl_3 .

NMR and measurements of the specific heat capacity (see Tab. II) give evidence for strong spin fluctuations also in the ordered phase of RbNiCl_3 . Figure 8 schematically shows the two basic spin relaxation mechanisms. Type I fluctuations are rotations of the spin-star around an axis perpendicular to the spin plane, i.e. parallel to the chirality vector $\vec{\kappa}$. This is the quasidegeneracy that has been discussed above. As indicated in the figure, these fluctuations preserve the chirality of the triangle; $\vec{\kappa}$ can still show long ranged order. All fluctuations with axis of rotation perpendicular to $\vec{\kappa}$ (Type II fluctuations) change the sign of $\vec{\kappa}$. If these fluctuations occur incoherently, $\vec{\kappa}$ cannot order. The phase transition should be of conventional type, as suggested by the LMB experiment.

Type II fluctuations seem not to depend directly on the Ising anisotropy D because the canting angle of the respective spins does not change during the rotation. Their incoherent occurrence in the ordered structure, however, may be emphasized by the presence of Type I fluctuations. when the Ising anisotropy is enlarged in CsNiCl_3 or in the $\text{RbNi}_{1-x}\text{Co}_x\text{Cl}$ system, the contribution of Type II fluctuations is obviously negligible, as these compounds show chiral ordering as predicted by theory. This seems to imply that Type II fluctuations play a major role only when Type I fluctuations are al-

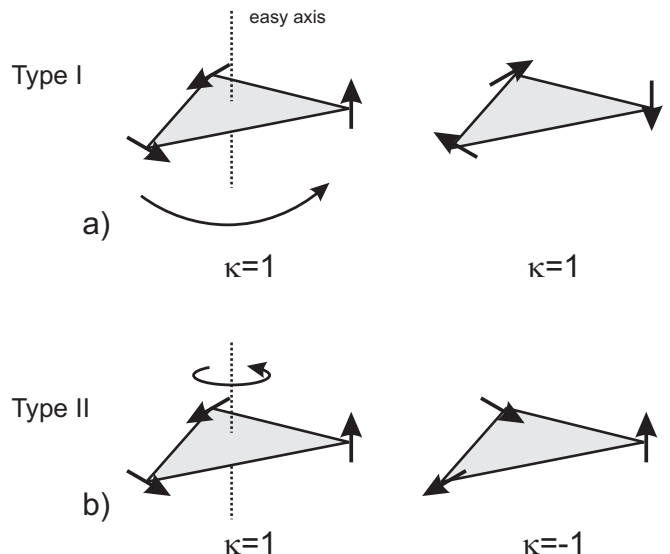


FIG. 8: Fluctuations of the triangle marked in Fig. 7: (a) Type I: Rotations about an axis parallel to the vector of chirality $\vec{\kappa}$ preserve the chirality. (b) Type II: Fluctuations around the easy-axis, perpendicular to $\vec{\kappa}$, change sign of the chirality.

ready strongly enhanced (as in pure RbNiCl_3).

The basic idea of fluctuations which on the one hand preserve (Type I) and on the other hand suppress (Type II) long ranged chiral order seems to account well for phase transitions and critical behavior observed in RbNiCl_3 . The separate ordering of the spin components parallel to the 1D axis, is presumably suppressed by Type I fluctuations; Type II fluctuations do not affect the projection of the magnetic moment onto the c -axis. But fluctuations of Type II might suppress ordering of the chirality $\vec{\kappa}$ at the phase transition T_N where the magnetic moment shows 3D ordering (whereas Type I fluctuations have no effect on the sign of $\vec{\kappa}$). If both types of fluctuations are strongly enhanced, we imagine that the domain walls between chirality domains of opposite sign move freely through the otherwise magnetically long-range ordered structure. If the chirality domain walls in the ordered phase behave liquid-like, the transition should show conventional Heisenberg critical behavior, as it is observed in the LMB experiment. In this language, the chirality domain walls in CsNiCl_3 or CsMnBr_3 are quasi-static. This liquid-like behavior of the domain walls, which leads to a different phase diagram and different critical behavior, as compared to other members of the ABX_3 family, must crucially depend on the almost perfect Heisenberg character of RbNiCl_3 .

V. CONCLUSIONS

We present a linear magnetic birefringence study in RbNiCl_3 . Our high resolution determination of the critical parameters α and the amplitude ratio A^+/A^- show conventional Heisenberg critical behavior like antiferro-

magnets on rectangular lattices (which have no ordered chirality) as opposed to theoretical predictions. There is just one phase transition in RbNiCl_3 . From a neutron diffraction study we can exclude a structural phase transition and a lift of the degeneracy of the magnetic exchange interactions in the basal plane at T_N . We discuss RbNiCl_3 in the framework of previous experimental and theoretical results and other members of the ABX_3 family. We finally argue that spin fluctuations lead to the unusual behavior of RbNiCl_3 . A separate phase transition of the spin component parallel to the easy-axis might be suppressed by spin fluctuations with axis of rotation parallel to the chirality vector $\vec{\kappa}$ (Type I fluctuations). Fluctuations of Type II, with axis of rotation perpendicular to $\vec{\kappa}$, presumably suppress long ranged order of the

chirality $\vec{\kappa}$ below T_N . The resulting single phase transition shows conventional Heisenberg critical behavior, as evidenced by the critical exponents and phase transitions observed in the LMB experiment.

Acknowledgments

We are indebted to and thank K. Knorr for hospitality and fruitful discussions. This work has been partially funded by the Universität des Saarlandes, Saarbrücken, Germany. We thank H. Tanaka for providing us with the high quality samples.

-
- * Present address: Institut Laue-Langevin, 6 rue Jules Horowitz, BP 156, 38042 Grenoble Cedex 9, France; Electronic address: rheinstaedter@ill.fr
- ¹ H. Kawamura, J. Appl. Phys. **61**, 3590 (1987).
 - ² M. Tissier, B. Delamotte, and D. Mouhanna, Phys. Rev. Lett. **84**, 5208 (2000).
 - ³ M. Collins and O. Petrenko, Can. J. Phys. **75**, 605 (1997).
 - ⁴ H. Kawamura, Phys. Soc. Jpn. **61**, 1299 (1992).
 - ⁵ H. Kawamura, Phys. Rev. B **47**, 3415 (1993).
 - ⁶ K. Nakajima, K. Kakurai, H. Hiraka, H. Tanaka, K. Iio, and Y. Endoh, J. Phys. Soc. Jpn. **61**, 3355 (1992).
 - ⁷ W. Yelon and D. Cox, Phys. Rev. B **6**, 204 (1972).
 - ⁸ Y. Oohara, H. Kadowaki, and K. Iio, J. Phys. Soc. Jpn. **60**, 393 (1991).
 - ⁹ K. Iio, H. Hyodo, and K. Nagata, J. Phys. Soc. Jpn. **49**, 1336 (1980).
 - ¹⁰ Y. Oohara, K. Iio, H. Tanaka, and K. Nagata, J. Phys. Soc. Jpn. **60**, 4280 (1991).
 - ¹¹ Y. Oohara and K. Iio, J. Phys. Soc. Jpn. **63**, 4597 (1994).
 - ¹² S. Muneta, S. Maegawa, A. Oyamada, T. Goto, and Y. Oohara, J. Magn. Magn. Mater. **140-144**, 1787 (1995).
 - ¹³ H. Tanaka, K. Nagata, and K. Iio, J. Magn. Magn. Mater. **104**, 829 (1992).
 - ¹⁴ H. Tanaka, T. Hasegawa, and K. Nagata, J. Phys. Soc. Jpn. **62**, 4053 (1993).
 - ¹⁵ P. Johnson, J. Rayne, and S. Friedberg, J. Appl. Phys. **50**, 1853 (1979).
 - ¹⁶ J. Rayne, J. Collins, and G. White, J. Appl. Phys. **52**, 1977 (1981).
 - ¹⁷ S. Collocot and J. Rayne, J. Appl. Phys. **61**, 4404 (1987).
 - ¹⁸ D. Beckmann, J. Wosnitza, and H. v. Löhneysen, Phys. Rev. Lett. **71**, 2829 (1983).
 - ¹⁹ H. Senarmont, Ann. Chim. Phys. **73**, 337 (1840).
 - ²⁰ D. Belanger, A. King, and V. Jaccarino, Phys. Rev. B **29**, 2636 (1984).
 - ²¹ J. Ferré and G. Gehring, Rep. Prog. Phys. **47**, 513 (1984).
 - ²² M. Zhitomirsky, O. Petrenko, and L. Prozorova, Phys. Rev. B **52**, 3511 (1995).
 - ²³ H. Kawamura, J. Appl. Phys. **63**, 3086 (1988).
 - ²⁴ S. Miyashita, J. Phys. Soc. Jpn. **55**, 3605 (1986).
 - ²⁵ S. Maegawa, T. Goto, and Y. Ajiro, J. Phys. Soc. Jpn. **57**, 1402 (1988).